HHS Public Access

Author manuscript

J Hepatol. Author manuscript; available in PMC 2022 October 01.

Published in final edited form as:

J Hepatol. 2021 October ; 75(4): 888–899. doi:10.1016/j.jhep.2021.05.018.

Focal Adhesion Kinase (FAK) promotes cholangiocarcinoma development and progression via YAP activation

Xinhua Song[1], **Hongwei Xu**[1,2], **Pan Wang**[1,3], **Jingxiao Wang**[4], **Silvia Affo**[5], **Haichuan Wang**[1,2], **Meng Xu**[6], **Binyong Liang**[7], **Li Che**[1,*], **Wei Qiu**[8], **Robert F Schwabe**[5], **Tammy T Chang**[9], **Marion Vogl**[10], **Giovanni M. Pes**[11], **Silvia Ribback**[12], **Matthias Evert**[10], **Xin Chen**[1], **Diego F. Calvisi**[10]

[1]Department of Bioengineering and Therapeutic Sciences and Liver Center, University of California, San Francisco, CA, USA

[2]Liver Transplantation Division, Department of Liver Surgery, West China Hospital, Sichuan University, Chengdu, China; Laboratory of Liver Surgery, West China Hospital, Sichuan University, Chengdu, Sichuan, People's Republic of China

[3]Collaborative Innovation Center for Agricultural Product Processing and Nutrition & Health, Beijing Vegetable Research Center, Beijing Academy of Agriculture and Forestry Science, Beijing, China

[4]Beijing University of Chinese Medicine, Beijing, China

[5]Department of Medicine, Columbia University, New York, NY, USA

[6]Department of General Surgery, The Second Affiliated Hospital of Xi'an Jiaotong University, Xi'an Jiaotong University, Xi'an, PR China

[7]Hepatic Surgery Center, Department of Surgery, Tongji Hospital, Tongji Medical College, Huazhong University of Science and Technology, Wuhan, China

[8]Department of Surgery and Cancer Biology, Loyola University Chicago Stritch School of Medicine, Maywood, IL

[9]Department of Surgery and Liver Center, University of California, San Francisco, CA, USA

[10]Institute of Pathology, University of Regensburg, Regensburg, Germany

Correspondence, proofs, and reprint requests to: Diego F. Calvisi, Institute of Pathology, University of Regensburg, Franz-Joseph-Strauss Allee 11, 93053 Regensburg, Germany; telephone: +49 941 944 6651; Fax: +49 941 944 6602; diego.calvisi@klinik.uni-regensburg.de or Xin Chen, UCSF, 513 Parnassus Avenue, San Francisco, CA 94143, USA; telephone: +1 415 502 6526; Fax: + 1 415 502 4322; xin.chen@ucsf.edu. Or Xinhua Song, UCSF, 513 Parnassus Avenue, San Francisco, CA 94143, USA; telephone: +1 415 502 6510; Fax: + 1 415 502 4322; songxinhua0726@yeah.net.

*Current address: R&D Center, Legend Biotech USA Inc, Piscataway, New Jersey, USA

Author Contributions: Xinhua Song, Hongwei Xu, Pan Wang, Jingxiao Wang, Silvia Affo, Haichuan Wang, Meng Xu, Binyong Liang, Marion Vogl, Giovanni M. Pes, Silvia Ribback, and Matthias Evert acquired experimental data. Li Che provided administrative, technical, or material support. Diego F. Calvisi, Xin Chen, Robert F Schwabe, Wei Qiu, and Tammy T Chang were involved in study design and obtaining funding.

Competing interests: The authors have no conflict of interest to disclose.

[11]Department of Medical, Surgical, and Experimental Sciences, University of Sassari, Sassari, Italy

[12]Institute of Pathology, University of Greifswald, Greifswald, Germany

Abstract

Background & Aims: Focal adhesion kinase (FAK) is a non-receptor tyrosine kinase upregulated in many tumor types and a promising target for cancer therapy. Here, we elucidated the functional role of FAK in intrahepatic cholangiocarcinoma (iCCA) development and progression.

Methods: Expression levels and activation status of FAK were determined in human iCCA samples. The functional contribution of FAK to *Akt/YAP* murine iCCA initiation and progression was investigated using conditional *Fak KO* mice and constitutive Cre or inducible Cre mice, respectively. The oncogenic potential of FAK was further examined via overexpression of FAK in mice. *In vitro* cell line studies and *in vivo* drug treatment were applied to address the therapeutic potential of targeting FAK for iCCA treatment.

Results: FAK was ubiquitously upregulated and activated in iCCA lesions. Ablation of FAK strongly delayed *Akt/YAP* driven mouse iCCA initiation. FAK overexpression synergized with activated AKT to promote iCCA development and accelerated *Akt/Jag1*-driven cholangiocarcinogenesis. Mechanistically, FAK was required for YAP(Y357) phosphorylation, supporting the role of FAK as a central YAP regulator in iCCA. Significantly, ablation of FAK after *Akt/YAP*-dependent iCCA formation strongly suppressed tumor progression in mice. Furthermore, a remarkable iCCA growth reduction was achieved when a FAK inhibitor and Palbociclib, a CDK4/6 inhibitor, were administered simultaneously in human iCCA cell lines and *Akt/YAP* mice.

Conclusions: FAK activation contributes to the initiation and progression of iCCA by inducing the YAP protooncogene. Targeting FAK, either alone or in combination with anti-CDK4/6 inhibitors, may be an effective strategy for iCCA treatment.

Lay summary

We found that Focal Adhesion Kinase (FAK) is upregulated and activated in human and mouse intrahepatic cholangiocarcinoma (iCCA) samples. FAK promotes iCCA development, whereas deletion of FAK strongly suppresses iCCA initiation and progression. Mechanistically, we discovered that FAK regulates the YAP pathway. Combined FAK and CDK4/6 inhibitor treatment is highly detrimental for the growth of *in vitro* and *in vivo* iCCA models. This combination therapy might represent a valuable and novel treatment against human iCCA.

Graphical Abstract

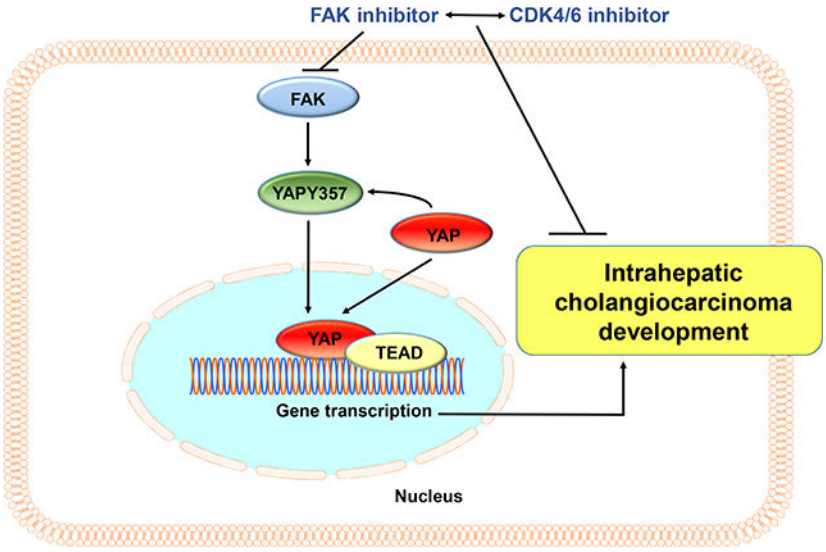

Keywords

intrahepatic cholangiocarcinoma; FAK; YAP; targeted therapy; iCCA

Introduction

Intrahepatic cholangiocarcinoma (iCCA) is the second most frequent primary liver tumor with few treatment options.[1] A detailed portrait and understanding of the molecular mechanisms leading to iCCA development and progression remain an unmet need.

Focal adhesion kinase (FAK), encoded by the *PTK2* gene, is a non-receptor protein tyrosine kinase.[2] Overexpression and activation of FAK are associated with the progression of many tumor types by modulating cell survival, proliferation, and invasion,[3] thus representing a promising target for cancer therapy.[4,5] Several FAK inhibitors have been tested in clinical trials, with preliminary results showing cytostatic effects as single agents.[5] Studies on the involvement of FAK in cholangiocarcinogenesis have been conducted previously.[6,7] However, comprehensive research on the role of FAK in iCCA development and progression is missing.

Yes-associated protein (YAP) is a main downstream effector of the Hippo pathway. YAP's cellular localization controls its activity: cytoplasmic YAP is indeed recruited to the disruption complex, ubiquitinated, and degraded,[8] whereas nuclear YAP induces gene transcription in association with the TEA domain transcription factor (TEAD) DNA binding proteins.[8,9] Previous studies demonstrated that the nuclear-cytoplasmic translocation of YAP depends on its phosphorylation status[8]. Specifically, YAP S127 and S397 sites are negative regulators of YAP nuclear localization, whereas phosphorylation at the Y357 (p-YAP^{Y357}) residue stabilizes YAP and promotes nuclear localization.[10] YAP plays a pivotal role in iCCA, where its overexpression and nuclear localization are ubiquitous.[11] Silencing of YAP inhibits iCCA cell growth *in vitro*,[12] and overexpression of the activated form of YAP, which is modified at 127 site (YapS127A) and cannot be targeted for proteasomal

degradation, cooperates with activated AKT to promote iCCA formation in mice.[11] Notably, several observations suggest that FAK mediates YAP nuclear translocation and induces its full activation.[13,14] The possible molecular crosstalk between FAK and YAP has not been investigated in iCCA.

Here, we evaluated FAK expression in human iCCA and its functional contribution to cholangiocarcinogenesis using *in vitro* and *in vivo* models.

Materials and Methods

Mouse experiments

Wild-type (WT) *FVB/N* mice were purchased from Charles River Laboratories (Wilmington, MA). *Fak*$^{f/f}$ mice were provided by Dr. Hilary Beggs (University of California San Francisco, San Francisco, CA), and *Yap*$^{f/f}$ mice by Dr. Eric Olson (University of Texas Southwestern Medical Center, Dallas, TX). Detailed information is available in Table S1. Mice were housed and monitored under protocols approved by the Committee for Animal Research, UCSF.

Statistical analysis

Data were analyzed using the Prism 8.0 software (GraphPad, San Diego, CA) and presented as Means ± SD. A two-tailed unpaired t-test was conducted to compare two groups that achieved Gaussian distribution, or a non-parametric test was performed when the sample size was small. Welch correction and linear regression were applied when necessary. Kaplan–Meier method and log-rank test were used for survival analysis. P values < 0.05 were considered statistically significant.

Additional detailed materials and methods are available in the Supporting document.

Results

FAK is upregulated and activated in human and *Akt/YAP* iCCA lesions

First, we analyzed the levels of the *PTK2* gene, encoding FAK, in the TCGA CHOL dataset.[15] Among 36 iCCA analyzed, 3 samples demonstrated *PTK2* amplification, and 1 harbored a missense mutation (H1033N) (Supplementary Figure 1A). *PTK2* mRNA levels were upregulated in iCCA samples compared to the surrounding non-tumorous liver tissues (Figure 1A). The results were independently validated in the NCI iCCA dataset (Figure 1A),[15,16], and our collection of human iCCA samples (Figure 2B). Using median expression as the cut-off, higher *PTK2* mRNA expression correlated with a lower iCCA survival rate (Figure 1C and Supplementary Tables 2–4). This association remained strongly significant after multivariate Cox regression analysis (Supplementary Table 5), supporting *PTK2* mRNA levels as a possible independent prognostic factor for iCCA. Using immunohistochemistry, positive immunoreactivity for total FAK and activated/phosphorylated (p-)FAK^{Y397} was detected in most iCCA samples (45/50 and 42/50, respectively). In contrast, a faint/absent staining for total and p-FAK^{Y397} characterized the non-tumorous surrounding livers (Supplementary Figures 2 and 3). Consistently, we

retrieved the FAK activation signature from KEGG (FOCAL),[17] and found that activation of the FAK signaling pathway is evident based on the TCGA CHOL dataset (Figure 1B).

Previously, we established a mouse iCCA model induced by hydrodynamic transfection of activated forms of AKT (myr-AKT) and YAP (YAPS127A) (*Akt/YAP*).[11] Using immunohistochemistry, p-FAK^{Y397} was readily detected in *Akt/YAP* iCCA lesions (Figure 1C). We performed RNASeq analysis of *Akt/YAP* iCCA (Figure 1D). Gene expression signature analysis confirmed FAK cascade's activation in *Akt/YAP* mouse iCCA (Figure 1D).

Altogether, the data demonstrate FAK activation in human and mouse iCCA.

FAK is required for iCCA growth *in vitro* and tumor initiation *in vivo*

We found that FAK is expressed in KKU-M213 and HuCC-T1 human iCCA cell lines. Culturing these cells on collagen triggered increased p-FAK^{Y397} levels (Supplementary Figure 4A). *PTK2* was silenced in the two cell lines using *shPTK2*, which effectively decreased FAK protein expression (Supplementary Figure 4B). FAK loss significantly suppressed the clonogenic capacity of both iCCA cell lines cultured in the two-dimensional culture matrix (Supplementary Figure 4B). Notably, *shPTK2* decreased iCCA cell growth in Collagen I 3D growth condition (Supplementary Figure 4C). Mechanistically, FAK ablation induced the expression of apoptosis-related protein cleaved caspase 3 (Supplementary Figure 4D) but did not affect proliferation-associated proteins, including p-Rb, PCNA, and Cyclin A/D1/E. Accordingly, PTK2 silencing via specific small-interfering RNA resulted in a mild decline of proliferation but a robust induction of apoptosis in KKU-M213 and HuCCT-1 cells (Supplementary Figure 5A–C). These data suggest FAK is required for human iCCA cell growth *in vitro,* mainly via apoptosis suppression.

To unravel the functional significance of FAK in the regulation of *Akt/YAP*-driven cholangiocarcinogenesis *in vivo*, we simultaneously deleted FAK while overexpressing AKT and YAP oncogenes in the mouse liver using FAK conditional KO ($Fak^{f/f}$) mice. In brief, *Akt* and *YAP* with pCMV-Cre (*Akt/YAP/Cre*) plasmids were injected into $Fak^{f/f}$ mice. As a control, additional $Fak^{f/f}$ mice were injected with *Akt/YAP* and *pCMV* empty vector (*Akt/YAP/pCMV*) (Figure 2A). In accordance with previous findings, [26] all control *Akt/YAP/pCMV* mice developed large abdominal masses and required euthanasia by 6–10 weeks post-injection. In striking contrast, loss of FAK strongly delayed *Akt/YAP*-driven liver tumor development. However, eventually all *Akt/YAP/Cre* injected $Fak^{f/f}$ mice became moribund and were harvested by 20 weeks post-injection (Figure 2B).

Grossly, when two cohorts of mice were harvested at 10 weeks post-injection, the liver tumor burden, estimated using total liver weight, was significantly lower in the *Akt/YAP/Cre* group (Figure 2C and 2D). Histologically, numerous tumor lesions occupied most of the liver parenchyma in *Akt/YAP/pCMV* mice at 10 weeks post-injection. At this time point, only small tumor lesions were appreciable instead in *Akt/YAP/Cre* mouse livers (Figure 2D). Western blot analysis confirmed FAK loss in *Akt/YAP/Cre* mice (Figure 2E).

Morphologically, *Akt/YAP/pCMV* tumors were classified as pure iCCA, as also substantiated by positive immunoreactivity for the biliary marker CK19 and negative immunolabeling for the hepatocellular marker HNF-4α (Figure 2F). Intriguingly, lesions consisted primarily of hepatic adenoma or HCC, but not iCCA, in *Akt/YAP/Cre* liver tissues. Even at 20 weeks post-injection, when large tumor lesions were present in *Akt/YAP/Cre* mouse livers, most lesions were HCC-like. This observation was confirmed by CK19 and HNF-4α immunohistochemistry (Figure 2F) and by qRT-PCR analysis of alpha-fetoprotein (*Afp*) and Glypican 3 (*Gpc3*) HCC markers (Figure 2G).

Loss of FAK did not affect liver tumor cell proliferation, as indicated by equal expression levels of PCNA and Cyclin A/B1/D1/E and Ki-67 immunohistochemistry in *Akt/YAP/pCMV* and *Akt/YAP/Cre* tumor lesions (Figure 2E and 2H). In contrast, cleaved caspase-3 levels significantly increased in *Akt/YAP/Cre* tumor tissues (Figure 2H), revealing augmented apoptosis in *Akt/YAP* lesions depleted of FAK.

Overall, the data indicate FAK requirement for iCCA *in vitro* growth and survival and *Akt/YAP*-induced iCCA formation *in vivo*. In these mice, loss of FAK delays tumor growth and alters the tumor phenotype.

FAK depletion represses YAP nuclear retention both *in vitro* and *in vivo*

Next, we investigated the mechanisms whereby FAK contributes to cholangiocarcinogenesis. YAP and one of its downstream effectors, the NOTCH pathway, play a pivotal role in biliary cell fate determination.[11,18] Previous studies suggested FAK as a driver of YAP nuclear translocation.[13,14] It is worth noting that in *Akt/YAP* induced iCCA model, we used the YAP (S127A) construct. There are additional phosphorylation sites of YAP, including YAP^{Y357}, which is necessary for YAP full activation.[19]

First, we tested whether FAK regulates YAP/NOTCH *in vitro*. Silencing of FAK in KKU-M213 and HuCC-T1 cells decreased nuclear YAP accumulation (Supplementary Figures 6A and 6B). Both sh*PTK2* and PND1186, a small FAK inhibitor, repressed p-YAP^{Y357} expression and decreased the levels of YAP target genes, as well as the downstream NOTCH pathway in these cells (Supplementary Figures 6 and 7). Other YAP phosphorylation sites, including p-YAP^{S127} and p-YAP^{S397}, did not show consistent changes.

In *Akt/YAP* mouse iCCA lesions, FAK deficiency did not affect the AKT or ERK signaling (Figure 3A and Supplementary Figure 8). Equivalent levels of ectopically expressed human *YAP1* mRNA were detected in both cohorts of mouse liver tissues (Figure 3B), indicating the successful expression of the human *YAP1* gene in these mice. In contrast, *Akt/YAP/Cre* tumors exhibited significantly lower total YAP and p-YAP^{Y357} levels (Figure 3A and Supplementary Figure 8). Immunohistochemistry revealed intense nuclear YAP staining in *Akt/YAP/pCMV* iCCA lesions. In *Akt/YAP/Cre* liver tumors, YAP expression was weaker, and both nucleus and cytoplasm staining was appreciable, with a significantly lower percentage of nuclear-only positive staining (Figure 3C). A decrease of YAP downstream targets, including SOX9, NOTCH2, and Jagged1 proteins, also occurred (Figure 3A and Supplementary Figure 8). Moreover, downregulation of canonical YAP targets (Figure 3D)

and NOTCH targets (Figure 3E) mRNA expression was observed in *Akt/YAP/Cre* tumor tissues.

We further investigated the FAK and YAP interplay in human iCCA specimens. Using immunohistochemistry, we detected the concomitant activation of FAK and YAP (as indicated by its nuclear accumulation) in most iCCA samples (37/50, 74%) (Supplementary Figure 2). Furthermore, a direct correlation between the mRNA levels of *PTK2* and YAP targets (*CTGF*, *CYR61*, *NOTCH2*, and *JAG1*), but not *YAP* mRNA, was detected (Supplementary Figure 9). The TCGA CHOL dataset revealed similar data (Supplementary Figure 10).

Overall, FAK ablation represses YAP activation by inhibiting p-YAP^{Y357}, leading to decreased YAP nuclear localization and activation. Simultaneous activation of FAK and YAP occurs in most human iCCA.

FAK overexpression synergizes with activated AKT to induce iCCA formation in mice

Next, we determined FAK oncogenic potential *in vivo*. Overexpression of FAK alone did not result in tumor development, consistent with previous findings.[20] Given that activated AKT synergizes with YAP to induce iCCA development, and FAK can activate YAP, we hypothesized that overexpression of FAK and AKT might trigger cholangiocarcinogenesis. To test this hypothesis, FAK and myr-AKT plasmids were co-injected into the mouse liver (*Akt/Fak* mice). Previously, we showed that overexpression of myr-AKT results in tumor development by 28 weeks post plasmid injection.[21] In *Akt/Fak* mice (Figure 4A), liver tumor nodules were detectable by ~15 weeks post-injection (Figure 4B). All mice developed a significant tumor burden and became moribund by 18–19 weeks post-injection (Figures 4B and 4C). Histologically, different from *Akt* mice, characterized almost exclusively by hepatocellular lesions,[21] *Akt/Fak* tumors displayed a solid and ductular phenotype resembling human iCCA (Figure 4B). All tumor cells were positive for CK19 and Ki-67 (Figure 4D). Western blotting confirmed that AKT and FAK pathways were successfully activated in *Akt/Fak* iCCAs (Figure 4E). Intense cytoplasmic and robust nuclear immunoreactivity for YAP was detected in *Akt/Fak* iCCA lesions (Figure 4D). Similarly, protein levels of YAP and related downstream targets Jagged1 and NOTCH2 were significantly induced (Figure 4E). The qRT-PCR analysis revealed that YAP target genes, including *Ctgf, Cyr61,* and *Axl*, and the NOTCH pathway's target genes (*Hes1* and *HeyL*), were upregulated in *Akt/Fak* tumors (Figure 4F).

Altogether, the present findings indicate that FAK overexpression cooperates with activated AKT to promote iCCA development, an event accompanied by YAP activation, in the mouse liver.

FAK overexpression accelerates *Akt/Jag1*-induced iCCA development in mice

Previously, we established an iCCA model by co-expressing myr-AKT and the Notch ligand Jag1 in the mouse liver (*Akt/Jag1* mice).[22] *Akt/Jag1* co-expression induces cystic-like iCCA lesions over long latency, characterized by low levels of YAP.[22] We hypothesized that overexpression of FAK might accelerate *Akt/Jag1*-driven cholangiocarcinogenesis by activating YAP. Thus, FAK was overexpressed in *AKT/Jag1* mice (*Akt/Jag1/Fak* mice).

Additional *AKT/Jag1* mice were injected with the pT3-EF1α empty vector as control (*Akt/Jag1/PT3*) (Figure 5A). Mice were harvested 10 weeks post-injection (Figure 5B). At this time point, liver tumor burden, estimated using total liver weight, was significantly higher in *Akt/Jag1/Fak* than in *Akt/Jag1/PT3* mice (Figure 5B). Both gross images and histological analysis revealed only small cystic nodules in *Akt/Jag1/PT3* mouse livers (Figure 5C), consistent with previous data.[22] In *Akt/Jag1/Fak* mice, tumors showed solid and ductal phenotypes, similar to those described in the *Akt/YAP* iCCA model (Figure 5C).[11] Tumor cells in both mouse cohorts were CK19 (+), with higher CK19 (+) areas in *Akt/Jag1/Fak* mice, supporting the higher iCCA burden (Figure 5C).

Mechanistically, FAK overexpression triggered increased iCCA cell proliferation (Figured 5D), with augmented expression of proliferation-related proteins, including CCND1 and PCNA (Figure 5E). Western blotting confirmed increased total and activated/phosphorylated FAK levels in *Akt/Jag1/Fak* tumor lesions (Figure 5E). Notably, while *Akt/Jag1/PT3* iCCA cells exhibited YAP cytoplasmic staining, intense cytoplasmic and nuclear YAP immunoreactivity characterized *Akt/Jag1/Fak* iCCA (Figure 5F). Nuclear accumulation of YAP was paralleled by increased p-YAP^{Y357} and NOTCH2 levels (Figure 5E). Moreover, the qRT-PCR analysis revealed an increased expression of YAP and NOTCH target genes in *Akt/Jag1/Fak* tumors (Figure 5G).

To determine whether *Akt/Jag1/Fak*-driven iCCA development is YAP dependent, *Akt/Jag1/Fak/pCMV* (control) and *Akt/Jag1/Fak/Cre* plasmids were injected in *Yap*$^{f/f}$ mice (Figure 5H). Nine weeks post-injection, all mice were harvested. Strikingly, *Yap* ablation completely suppressed iCCA formation in *Akt/Jag1/Fak* mice at this time point (Figures 5I and 5J). While *Akt/Jag1/Fak/Cre* injected *Yap*$^{f/f}$ mice were healthy with no macroscopic liver nodules, all *Akt/Jag1/Fak/pCMV* injected mice exhibited a high tumor burden. Histological analysis revealed iCCA lesions in *Akt/Jag1/Fak/pCMV* injected mouse livers. In contrast, no malignant lesions developed in *Akt/Jag1/Fak/Cre* livers, where hepatocytes with enlarged clear cytoplasm owing to increased fat and glycogen storage induced by AKT activation were detected (Figure 5J).[21]

Overall, the data indicate that FAK overexpression accelerates *Akt/Jag1*-driven cholangiocarcinogenesis in a YAP-dependent manner.

iCCA progression *in vivo* requires an intact FAK

To assess the therapeutic potential of targeting FAK for iCCA treatment, we determined whether FAK ablation after *Akt/YAP* iCCA formation triggers tumor regression. Thus, we generated a sleeping beauty transposase-based vector with Tamoxifen-inducible Cre, i.e., CreER^{T2,} under the control of the CK19 promoter (pT3-CK19pro-CreER^{T2}) (Supplementary Figure 11A). The pT3-CK19pro-CreER^{T2} plasmid together with AKT and YAP constructs was injected into *Fak*$^{f/f}$ mice. Mice were aged until ~3.5 to 4 weeks post-injection when iCCA tumors are appreciable on the mouse surface (Figure 6A and Supplementary Figure 11B). A group of mice was harvested as a pretreatment cohort, and additional mice were either intraperitoneally injected with corn oil (control) or Tamoxifen (Supplementary Table 6). Tamoxifen administration allows the activation of the Cre recombinase and the subsequent deletion of FAK only in CK19(+) iCCA tumor cells. Significantly, deletion

of FAK in *Akt/YAP* lesions profoundly inhibited tumor progression (Figure 6B). Indeed, while all corn oil-injected mice required euthanasia by 5–10 weeks post hydrodynamic injection, Tamoxifen-treated mice survived considerably longer (Figure 6B). In total, 10 *Akt/YAP/CreER^{T2}* mice were treated with Tamoxifen (Supplementary Table 6). Four mice (Group 1) developed a significant liver tumor burden and required euthanasia by 11–15 weeks post-injection (Figure 6C and Supplementary Figure 11B). Additional 6 mice (Group 2) appeared to be healthy, with 3 exhibiting low tumor burden when harvested at 10 weeks post-injection. The remaining 3 mice demonstrated low tumor burden even 17–20 weeks after hydrodynamic injection (Figures 6B and 6C). Upon dissection, limited tumor burden was observed in this mouse cohort. Indeed, few tumors were detected, and most lesions consisted of small cell clusters (Figure 6D and Supplementary Figure 11B). When assessing FAK by Western blotting, we found similar FAK levels in control and Tamoxifen-treated Group 1 mice (Figure 6E). In contrast, FAK protein was significantly decreased in Group 2 mice (Figure 6E). The results indicate that Tamoxifen failed to induce sufficiently elevated Cre activity in Group 1 mice, leading to the continuous growth of the iCCA lesions retaining FAK expression. To rule out the possibility that Tamoxifen treatment was responsible for the impaired tumor progression, we injected FVB/N mice with *Akt/YAP/CreER^{T2}* and repeated the experiments (Supplementary Figure 11C). As expected, Tamoxifen treatment did not trigger tumor growth inhibition in wild-type mice.

We focused our analysis on Group 2 mice, demonstrating efficient Cre-mediated FAK deletion. Histological analysis and CK19 immunohistochemistry showed that *Akt/YAP* mice after Tamoxifen treatment displayed a lower tumor burden than pretreatment mice (Figure 6D). FAK ablation after iCCA formation did not result in HCC-like conversion of the lesions (Figure 6D). Notably, large areas of necrosis were detected only in Tamoxifen-treated livers (Figure 6F). YAP immunohistochemistry revealed nuclear YAP staining in iCCA lesions, indicating the preservation of YAP activity in these residual iCCA lesions after FAK deletion (Supplementary Figure 11D).

Altogether, the present data demonstrate that FAK ablation in already formed iCCA inhibits tumor progression, implying FAK as a potentially relevant therapeutic target in iCCA.

Combined FAK and CDK4/6 inhibition is detrimental for iCCA growth *in vitro* and *in vivo*

To explore FAK as a therapeutic target for iCCA treatment, we treated the KKU-M213 and HuCC-T1 cells with PND1186, a FAK inhibitor. PND1186 effectively inhibited the cell growth of both cell lines with an IC_{50} of 4.47μM and 11.1μM, respectively (Supplementary Figures 12A). We reasoned that FAK inhibitors might have limited efficacy for cancer treatment as single agents. Based on our RNASeq analysis of *Akt/YAP* murine iCCA treated with various drugs, Oxaliplatin/Gemcitabine combination[11], MLN0128[11], and Palbociclib[23] treatment had no substantial influence on FAK pathway enrichment in *Akt/YAP* tumors (Supplementary Figures 1B and 1C). Therefore, FAK inhibitors may synergize with one of these drugs, leading to more substantial tumor growth suppression. Previously, we showed the CDK4/6 pathway activation in mouse and human iCCA. The CDK4/6 inhibitor Palbociclib profoundly suppressed iCCA cell proliferation *in vitro*.[23] Moreover, most human iCCA samples examined (35/50, 70%) displayed concomitant immunoreactivity for

activated FAK and phosphorylated/inactivated (p-)pRb, a reliable marker of CDK4/6 activity and response to CDK4/6 inhibitors (Supplementary Figure 13).[24] We hypothesized that FAK and anti-CDK4/6 inhibitors might synergize against iCCA. Thus, KKU-M213 and HuCC-T1 cells were treated with Palbociclib and PND1186, either alone or in combination. Compared to single treatments, concomitant administration of Palbociclib and PND1186 to iCCA cells induced decreased cell viability (Supplementary Figures 12B). The combination index (CI) was calculated,[25] and all CI values were less than 1 in Palbociclib and PND1186 treatment groups (Supplementary Figure 12C and D), indicating a synergistic anti-tumor activity of Palbociclib/PND1186 co-administration. This assumption was confirmed by assessing proliferation and apoptosis rates in the same cell lines. Indeed, the Palbociclib/PND1186-treated cohort showed the highest reduction in proliferation and massive apoptosis in KKU-M213 and HuCC-T1 cells (Supplementary Figure 14A–D). Notably, PND1186 alone displayed a significantly higher pro-apoptotic potential than Palbociclib in both cell lines (Supplementary Figure 14C and D).

Subsequently, we tested the therapeutic potential of FAK inhibitor, either alone or in combination with Palbociclib, in the *Akt/YAP* iCCA model. We selected VS-6063 (defactinib) as the FAK inhibitor since it is orally bioavailable and currently tested in clinical trials for cancer therapy.[26] Treatment with Palbociclib (100mg/kg) and VS-6063 (50mg/kg) was well-tolerated in mice. *Akt/YAP* tumor-bearing mice were randomly separated into 5 cohorts (Figure 7A). The first group was harvested 4.5 weeks post hydrodynamic injection as the pretreatment group. All mice exhibited moderate iCCA liver tumor burden at this point, with an average liver weight of ~2.5g. The remaining mice were treated with vehicle, VS-6063, Palbociclib, or VS-6063/Palbociclib for 3 weeks. All mice developed large tumors in the vehicle treatment cohort and were euthanized by 6.5 to 7.5 weeks post-injection (Figure 7B). VS-6063 or Palbociclib treated mice exhibited a slower but still progressive tumor growth, indicated by the lower tumor burden than the vehicle cohort but higher tumor burden than the pretreatment cohort (Figure 7C). Strikingly, VS-6063/Palbociclib combination therapy exhibited a strong anti-neoplastic effect with the lowest liver weight (Figure 7C). No differences in liver weight between the pretreatment and combination therapy groups were detected (Figure 7C). Histologically, iCCA lesions were identified in all cohorts (Figure 7C). Using CK19-positive tumor area as a second measurement of iCCA tumor burden in mice, we confirmed that either VS-6063 or Palbociclib treatment resulted in slower but progressive disease. Combined VS-6063/Palbociclib was effective against *Akt/YAP* iCCA, leading to decreased tumor burden in mice compared with single treatment groups and the pretreatment cohort (Figure 7C and Supplementary Figure 15). Similar effects were detected when looking at tumor area percentage. Indeed, the combination treatment reduced the tumor burden significantly even compared with the pretreatment cohort (Figure 7C, Supplementary Figure 15).

At the cellular level, VS-6063 or Palbociclib treatment mildly decreased Ki-67(+) positive cells, whereas the combination treatment more potently suppressed tumor cell proliferation (Figure 7C). In terms of apoptosis, VS-6063 administration induced apoptosis in iCCA lesions, and the combination treatment resulted in a further increase in cell death. Previous studies suggest the FAK modulates cancer-associated fibroblasts (CAFs) and fibrosis during

tumor progression[27]. Using immunostaining with the anti-Vimentin antibody, we found that VS-6063 treatment did not affect CAFs in the mouse lesions (Supplementary Figure 16).

At the molecular level, VS-6063 was effective in suppressing p-FAK, Palbociclib strongly inhibited p-Rb, and the combination treatment increased the apoptosis marker cleaved caspase-3. Notably, consistent with the *in vitro* and *in vivo* data, VS-6063-mediated FAK inhibition downregulated the levels of YAP-related effectors (JAG1, NOTCH2, and HES1) (Supplementary Figure 17).

Overall, the data indicate that FAK targeting combined with CDK4/6 inhibitors induces tumor regression in *Akt/YAP* mice and might be an effective therapy for human iCCA.

Discussion

Here, we demonstrate that FAK is strongly activated in most human iCCA specimens. The precise mechanisms responsible for FAK activation in iCCA remain undefined. iCCA is a tumor characterized by a high desmoplastic reaction, whose components functionally interact with iCCA cells.[28] Thus, it would be essential to determine whether the tumor microenvironment induces the activation of FAK in iCCA and, if so, which is the primary cell type responsible for this event.

To investigate FAK functional role in iCCA development, we applied the *Akt/YAP* iCCA murine model,[11] as we detected FAK activation in *Akt/YAP* iCCA lesions. In this model, two sets of experiments were conducted. In the first set, we deleted FAK during tumor initiation in *Akt/YAP* mice. FAK deletion resulted in a significant delay of *Akt/YAP*-dependent iCCA formation. In the second set of experiments, the cholangiocyte-specific inducible Cre system combined with conditional *Fak* KO mice was employed. This strategy allowed FAK deletion in *Akt/YAP* iCCA after tumor formation to investigate FAK requirement for iCCA progression. Our study shows that FAK deletion after iCCA initiation significantly inhibited *Akt/YAP*-driven iCCA development. Besides, we demonstrated that FAK ablation promoted apoptosis. Further studies are required to address how FAK overexpression suppresses tumor cell apoptosis. These findings support the crucial role of FAK during both iCCA initiation and progression.

Mechanistically, we discovered that FAK induces YAP phosphorylation at the Y357 residue, thus promoting YAP activation in iCCA cell lines and mouse models. Notably, FAK also caused the increase of p-YAP^{S397} levels, implying inhibition of the YAP pathway. This contradicting observation might be the result of multiple feedback mechanisms in response to YAP activation.[29] Moreover, we discovered that FAK ablation does not affect *Akt/Nicd*-driven cholangiocarcinogenesis as YAP lies upstream of NOTCH (Supplementary Figure 18). Also, it is worth noting that when deletion of *Fak* occurred in already formed *Akt/YAP* iCCA tumors, YAP activity was preserved in the residual iCCA tumor nodules. Presumably, additional FAK-independent mechanisms maintain YAP activation and sustain the proliferation of iCCA cells in *Fak*-deleted tumor cells.

The present findings have important translational implications. Indeed, we demonstrated that FAK inhibitors combined with CDK4/6 inhibitors potently inhibited iCCA growth both *in*

vitro and *in vivo*. The relevance of this drug combination strategy is further supported by the simultaneous activation of FAK and CDK4/6 cascades in over 70% of human iCCA samples. The results open the door for testing this combination therapy for iCCA treatment in clinical trials.

Supplementary Material

Refer to Web version on PubMed Central for supplementary material.

Acknowledgments

We thank Dr. Hilary Beggs at the University of California, San Francisco, for $Fak^{f/f}$ mice; and Dr. Eric Olson from the University of Texas Southwestern Medical Center, for $Yap^{f/f}$ mice.

Financial Support Statement: This work was supported by NIH grants R01CA190606 and R03CA288375 to XC; R01CA228483 to XC, TC, and RFS; R01CA197128 to WQ; and P30DK026743 for UCSF Liver Center.

Data availability:

The data that support the findings of this study are included within the article and its supplementary materials.

List of Abbreviations:

AFP
α-fetoprotein

AKT
v-akt murine thymoma viral oncogene homolog

CAF
cancer-associated fibroblasts

Chemo
Oxaliplatin/Gemcitabine combination

FAK
Focal adhesion kinase

FOCAL
focal adhesion pathway

Gpc3
Glypican 3

H&E
Hematoxylin-Eosin staining

HNF4α
Hepatocyte nuclear factor 4α

HTVi
Hydrodynamic tail vein injection

iCCA
intrahepatic cholangiocarcinoma

KO
Knockout

MLN
MLN0128

MP
MLN0128/Palbociclib combination

Palbo
Palbociclib

Pre
Pretreatment

qRT-PCR
quantitative reverse transcription PCR

NCI
National Cancer Institute

SB
Sleeping beauty

TCGA
The Cancer Genome Atlas

TEAD
TEA domain transcription factor

YAP
Yes-associated protein

WT
Wild-type

IHC
immunohistochemistry

W.P.I.
weeks post-injection

Sac
sacrifice

References

Author names in bold designate shared co-first authorship.

1. Rizvi S, Khan SA, Hallemeier CL, Kelley RK, Gores GJ. Cholangiocarcinoma - evolving concepts and therapeutic strategies. Nature reviews Clinical oncology2018;15:95–111.
2. Sulzmaier FJ, Jean C, Schlaepfer DD. FAK in cancer: mechanistic findings and clinical applications. Nature reviews Cancer2014;14:598–610. [PubMed: 25098269]
3. Panera N, Crudele A, Romito I, Gnani D, Alisi A. Focal Adhesion Kinase: Insight into Molecular Roles and Functions in Hepatocellular Carcinoma. International journal of molecular sciences2017;18;99.
4. Lee BY, Timpson P, Horvath LG, Daly RJ. FAK signaling in human cancer as a target for therapeutics. Pharmacology & therapeutics2015;146:132–149. [PubMed: 25316657]
5. Mohanty A, Pharaon RR, Nam A, Salgia S, Kulkarni P, Massarelli E. FAK-targeted and combination therapies for the treatment of cancer: an overview of phase I and II clinical trials. Expert opinion on investigational drugs2020;29:399–409. [PubMed: 32178538]
6. Mon NN, Hasegawa H, Thant AA, Huang P, Tanimura Y, Senga T, et al.A role for focal adhesion kinase signaling in tumor necrosis factor-alpha-dependent matrix metalloproteinase-9 production in a cholangiocarcinoma cell line, CCKS1. Cancer research2006;66:6778–6784. [PubMed: 16818654]
7. Pongchairerk U, Guan JL, Leardkamolkarn V. Focal adhesion kinase and Src phosphorylations in HGF-induced proliferation and invasion of human cholangiocarcinoma cell line, HuCCA-1. World journal of gastroenterology2005;11:5845–5852. [PubMed: 16270396]
8. Rausch V, Hansen CG. The Hippo Pathway, YAP/TAZ, and the Plasma Membrane. Trends in cell biology2020;30:32–48. [PubMed: 31806419]
9. Nguyen CDK, Yi C. YAP/TAZ Signaling and Resistance to Cancer Therapy. Trends in cancer2019;5:283–296. [PubMed: 31174841]
10. Zhao B, Li L, Tumaneng K, Wang CY, Guan KL. A coordinated phosphorylation by Lats and CK1 regulates YAP stability through SCF(beta-TRCP). Genes & development2010;24:72–85. [PubMed: 20048001]
11. Zhang S, Song X, Cao D, Xu Z, Fan B, Che L, et al.Pan-mTOR inhibitor MLN0128 is effective against intrahepatic cholangiocarcinoma in mice. Journal of hepatology2017;67:1194–1203. [PubMed: 28733220]
12. Sugihara T, Isomoto H, Gores G, Smoot R. YAP and the Hippo pathway in cholangiocarcinoma. 2019;54:485–491.
13. Lachowski D, Cortes E, Robinson B, Rice A, Rombouts K, Del Río Hernández AE. FAK controls the mechanical activation of YAP, a transcriptional regulator required for durotaxis. FASEB journal : official publication of the Federation of American Societies for Experimental Biology2018;32:1099–1107. [PubMed: 29070586]
14. Kim NG, Gumbiner BM. Adhesion to fibronectin regulates Hippo signaling via the FAK-Src-PI3K pathway. The Journal of cell biology2015;210:503–515. [PubMed: 26216901]
15. Farshidfar F, Zheng S, Gingras MC, Newton Y, Shih J, Robertson AG, et al.Integrative Genomic Analysis of Cholangiocarcinoma Identifies Distinct IDH-Mutant Molecular Profiles. Cell reports2017;18:2780–2794. [PubMed: 28297679]
16. Andersen JB, Spee B, Blechacz BR, Avital I, Komuta M, Barbour A, et al.Genomic and genetic characterization of cholangiocarcinoma identifies therapeutic targets for tyrosine kinase inhibitors. Gastroenterology2012;142:1021–1031 e1015. [PubMed: 22178589]
17. Gao X, Chen Y, Chen M, Wang S, Wen X, Zhang S. Identification of key candidate genes and biological pathways in bladder cancer. PeerJ2018;6:e6036. [PubMed: 30533316]
18. Zhang S, Zhou D. Role of the transcriptional coactivators YAP/TAZ in liver cancer. Current opinion in cell biology2019;61:64–71. [PubMed: 31387016]
19. Li B, He J, Lv H, Liu Y, Lv X, Zhang C, et al.c-Abl regulates YAPY357 phosphorylation to activate endothelial atherogenic responses to disturbed flow. The Journal of clinical investigation2019;129:1167–1179. [PubMed: 30629551]

20. Shang N, Wang H, Bank T, Perera A, Joyce C, Kuffel G, et al.Focal Adhesion Kinase and β-Catenin Cooperate to Induce Hepatocellular Carcinoma. Hepatology2019;70:1631–1645. [PubMed: 31069844]
21. Calvisi DF, Wang C, Ho C, Ladu S, Lee SA, Mattu S, et al.Increased lipogenesis, induced by AKT-mTORC1-RPS6 signaling, promotes development of human hepatocellular carcinoma. Gastroenterology2011;140:1071–1083. [PubMed: 21147110]
22. Che L, Fan B, Pilo MG, Xu Z, Liu Y, Cigliano A, et al.Jagged 1 is a major Notch ligand along cholangiocarcinoma development in mice and humans. Oncogenesis2016;5:e274. [PubMed: 27918553]
23. Song X, Liu X, Wang H, Wang J, Qiao Y, Cigliano A, et al.Combined CDK4/6 and Pan-mTOR Inhibition Is Synergistic Against Intrahepatic Cholangiocarcinoma. Clinical cancer research2019;25:403–413. [PubMed: 30084835]
24. Schettini F, De Santo I, Rea CG, De Placido P, Formisano L, Giuliano M, et al.CDK 4/6 Inhibitors as Single Agent in Advanced Solid Tumors. Frontiers in oncology2018;8:608. [PubMed: 30631751]
25. Chou TC. Theoretical basis, experimental design, and computerized simulation of synergism and antagonism in drug combination studies. Pharmacological reviews2006;58:621–681. [PubMed: 16968952]
26. Gerber DE, Camidge DR, Morgensztern D, Cetnar J, Kelly RJ, Ramalingam SS, et al.Phase 2 study of the focal adhesion kinase inhibitor defactinib (VS-6063) in previously treated advanced KRAS mutant non-small cell lung cancer. Lung cancer (Amsterdam, Netherlands)2020;139:60–67.
27. Jiang H, Liu X, Knolhoff BL, Hegde S. Development of resistance to FAK inhibition in pancreatic cancer is linked to stromal depletion. Gut2020;69:122–132. [PubMed: 31076405]
28. Vaquero J, Aoudjehane L, Fouassier L. Cancer-associated fibroblasts in cholangiocarcinoma. Current opinion in gastroenterology2020;36:63–69. [PubMed: 31934895]
29. Moroishi T, Park HW, Qin B, Chen Q, Meng Z, Plouffe SW, et al.A YAP/TAZ-induced feedback mechanism regulates Hippo pathway homeostasis. Genes & development2015;29:1271–1284. [PubMed: 26109050]

Highlights

- FAK is activated in human and mouse intrahepatic cholangiocarcinoma (iCCA) samples.
- Overexpression of FAK promotes cholangiocarcinogenesis, whereas deletion of FAK strongly suppresses iCCA initiation and progression.
- FAK modulates YAP nuclear localization via phosphorylating YAP at the Y357 residue to promote iCCA development.
- FAK is a potential therapeutic target for human iCCA treatment.

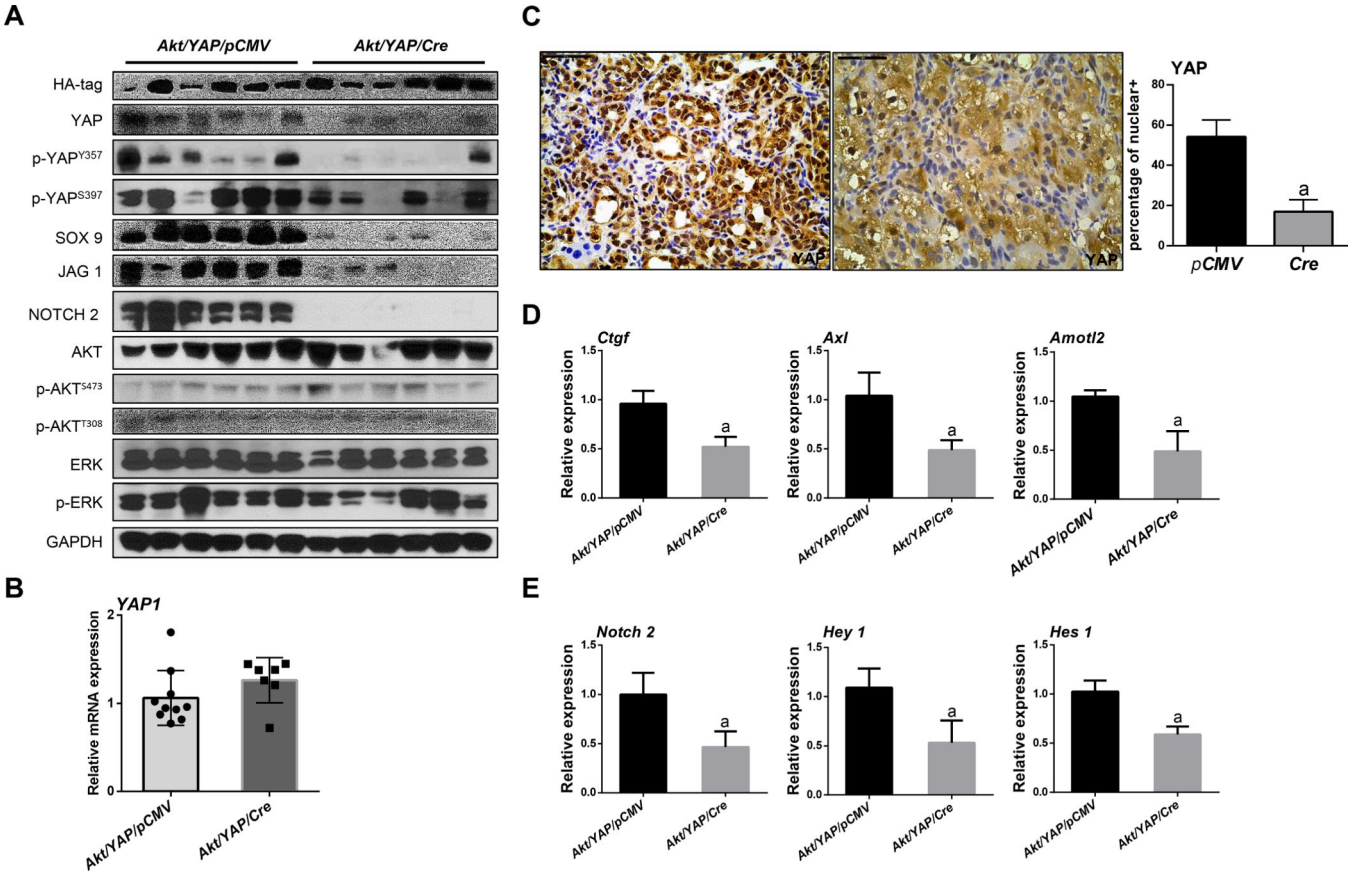

Figure 1. FAK is activated in human iCCA patients and *Akt/YAP*-induced iCCA mouse lesions.

(A) *PTK2* mRNA levels in human intrahepatic cholangiocarcinoma (iCCA) from The Cancer Genome Atlas (TCGA) and National Cancer Institute (NCI) datasets. (B) Quantitative real-time RT-PCR analysis of *PTK2* expression in iCCA (n = 50) and corresponding non-tumorous surrounding liver tissues (ST; n = 50) from our cohort. (C) Kaplan–Meier survival curves of human iCCA specimens from our cohort with high and low *PTK2* mRNA levels, showing the unfavorable outcome of patients with elevated expression of this gene. (D) GSEA analysis of FAK pathway-related proteins in iCCA from TCGA. (E-F) FAK activation in the *Akt/YAP*-induced iCCA mouse model.

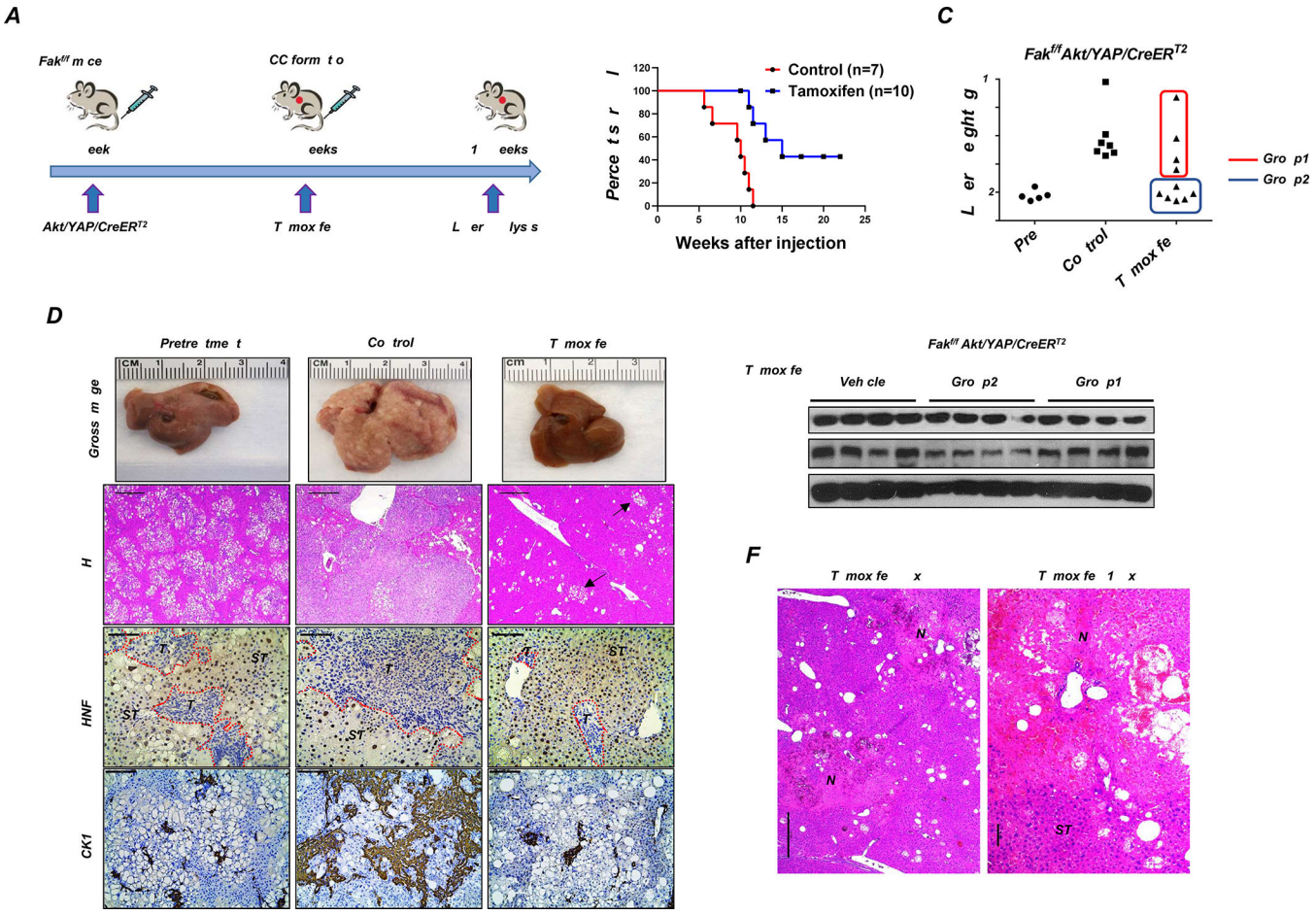

Figure 2. Deletion of FAK suppresses iCCA development in *Akt/YAP* mice.

(A) Study design. (B) Survival analysis of *Fak*$^{f/f}$ mice bearing *Akt/YAP/pCMV* (n =15) and *Akt/YAP/Cre* (n = 10) tumors. (C) Liver weight of *Akt/YAP/pCMV* and *Akt/YAP/Cre* mice at 10 weeks post hydrodynamic injection. (D) Gross image and H&E staining of *Akt/YAP/pCMV* and *Akt/YAP/Cre* mouse livers. (E) Western blot analysis of iCCA tissues from *Akt/YAP-pCMV* and *Cre Fak*$^{f/f}$ mice. GAPDH was the loading control. (F) H&E and IHC staining of CK19 and HNF-4α in *Akt/YAP/pCMV* and *Akt/YAP/Cre Fak*$^{f/f}$ mice, respectively. CK19 staining was quantified as the percentage of the positive staining area of the whole tumor section area. HNF-4α positive cells were quantified as HNF-4α index. (G) Relative mRNA expressions of *AFP* and *GPC3* were analyzed using the −ΔΔCt method and presented as mean ± SD. (H) Immunohistochemistry of Ki-67 and C-C-3 was performed in *Akt/YAP/pCMV* and *Akt/YAP/Cre Fak*$^{f/f}$ mice. Ki-67 and C-C-3 positive cells were quantified using the Image J. Tukey–Kramer test: at least $P < 0.005$; a, vs. *Akt/YAP/pCMV*; b, vs. *Akt/YAP/Cre*. Abbreviations: C-C-3, Cleaved Caspase 3; T, tumor; ST, surrounding tissue. Scale bar: 100 μm for 200×.

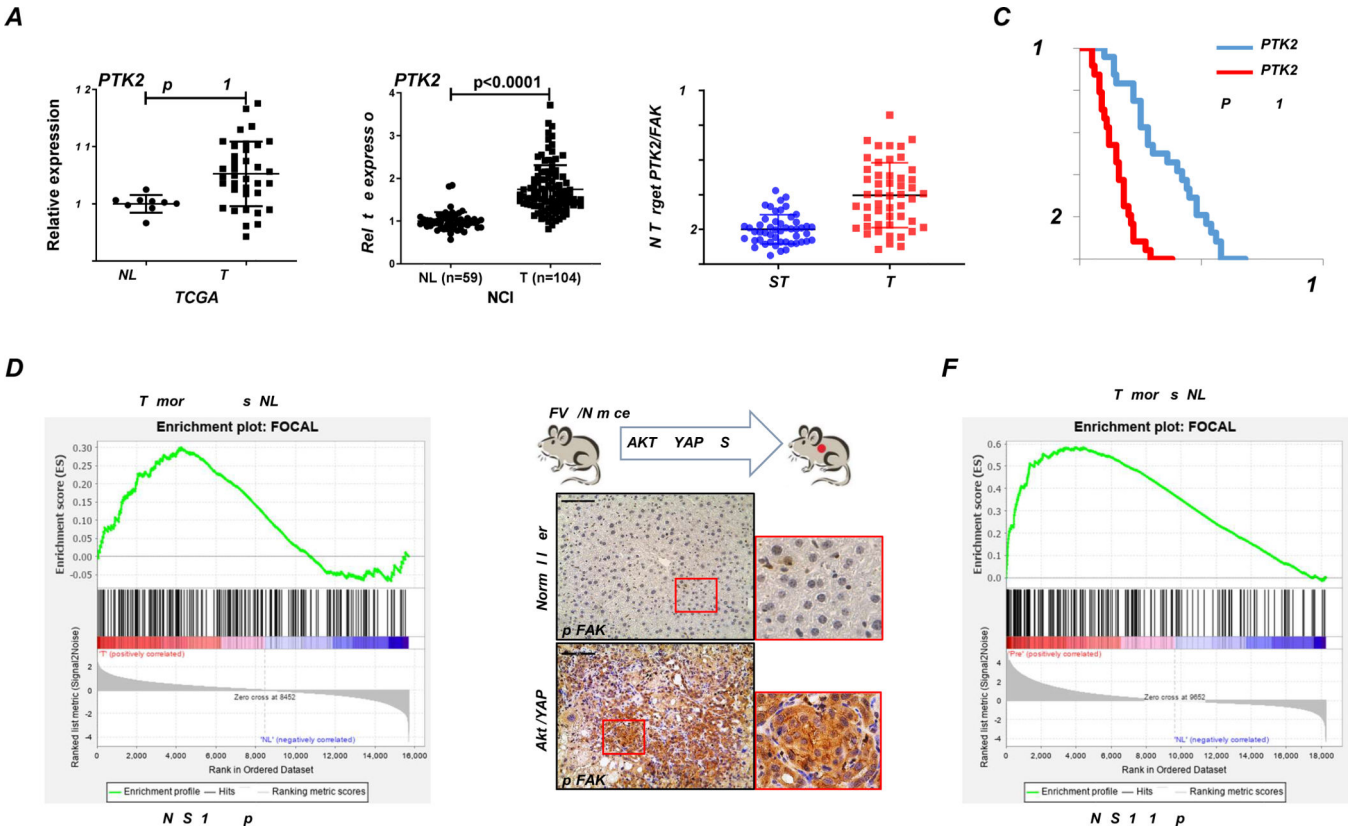

Figure 3. YAP signaling inactivation in iCCA from FAK conditional knockout *Akt/YAP* mice.

(A) Western blot analysis of lysates from *Akt/YAP/pCMV* and *Akt/YAP/Cre Fak*$^{f/f}$ mice. (B) Levels of human *Yap1* mRNA in *Akt/YAP/pCMV* and *Akt/YAP/Cre* mice. (C) Knockout of FAK reduced YAP nuclear translocation as shown by immunohistochemistry and the percentage of positive nuclear staining. (D) YAP and (E) NOTCH signaling inactivation at the transcriptional level, as assessed by qPCR. Tukey–Kramer test: at least P < 0.05; a, vs *Akt/YAP-pCMV*; b, vs *Akt/YAP-Cre*.

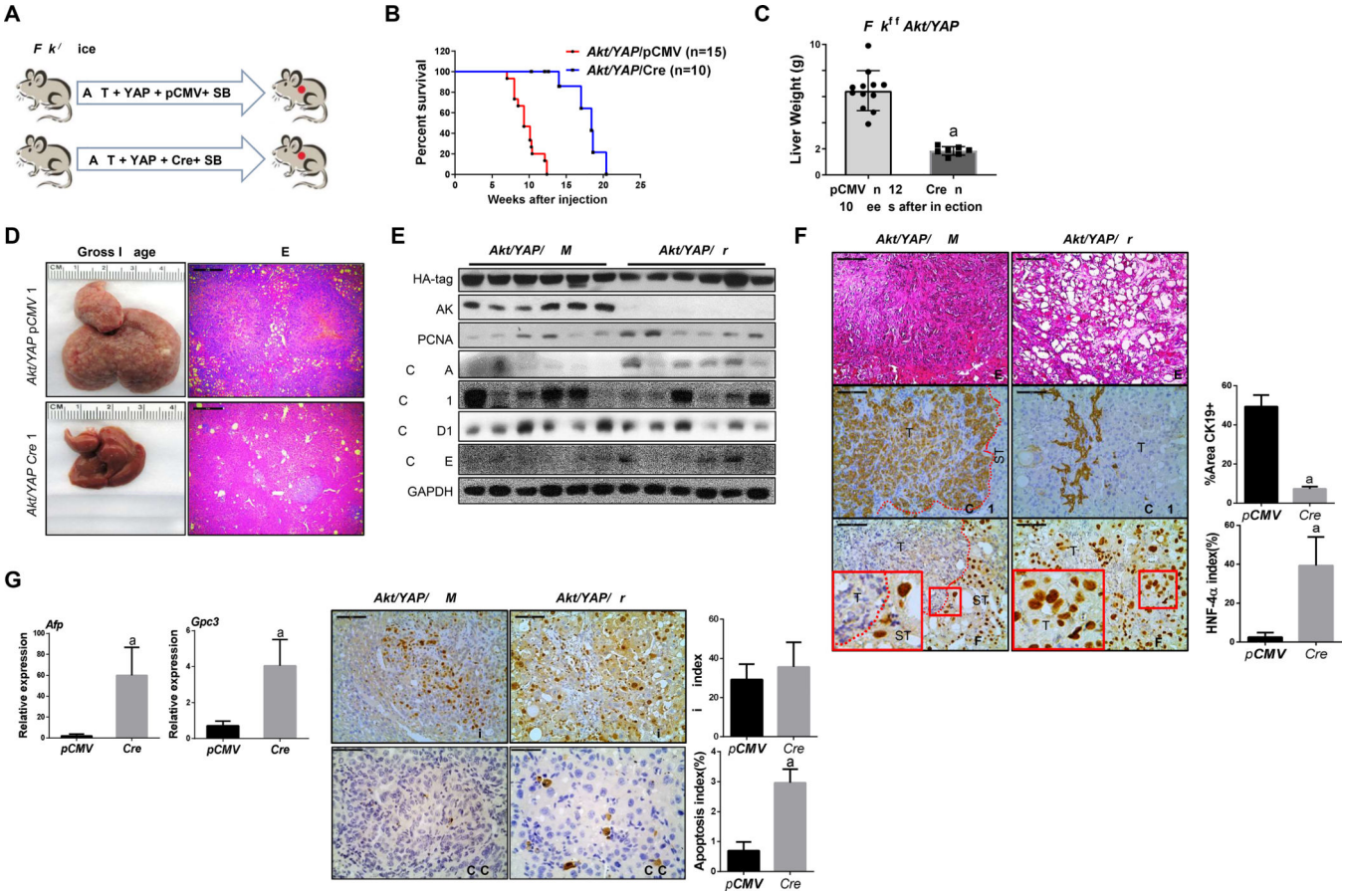

Figure 4. Co-expression of FAK and AKT leads to iCCA formation in mice.

(A) Study design. (B) Gross image and H&E staining of *Akt/Fak* mouse livers. (C) Liver weight of *Akt/Fak* mice at 18–19 weeks post-injection. (D) Immunohistochemistry of CK19, Ki-67, and YAP in *Akt/Fak* mice. (E) Western blot analysis of FVB mice and *Akt/Fak* mouse model liver tissues. (F) YAP and NOTCH signaling activation at the transcriptional level, as assessed by qPCR. Tukey–Kramer test: at least $P < 0.05$; a, vs FVB WT; b, vs *Akt.*

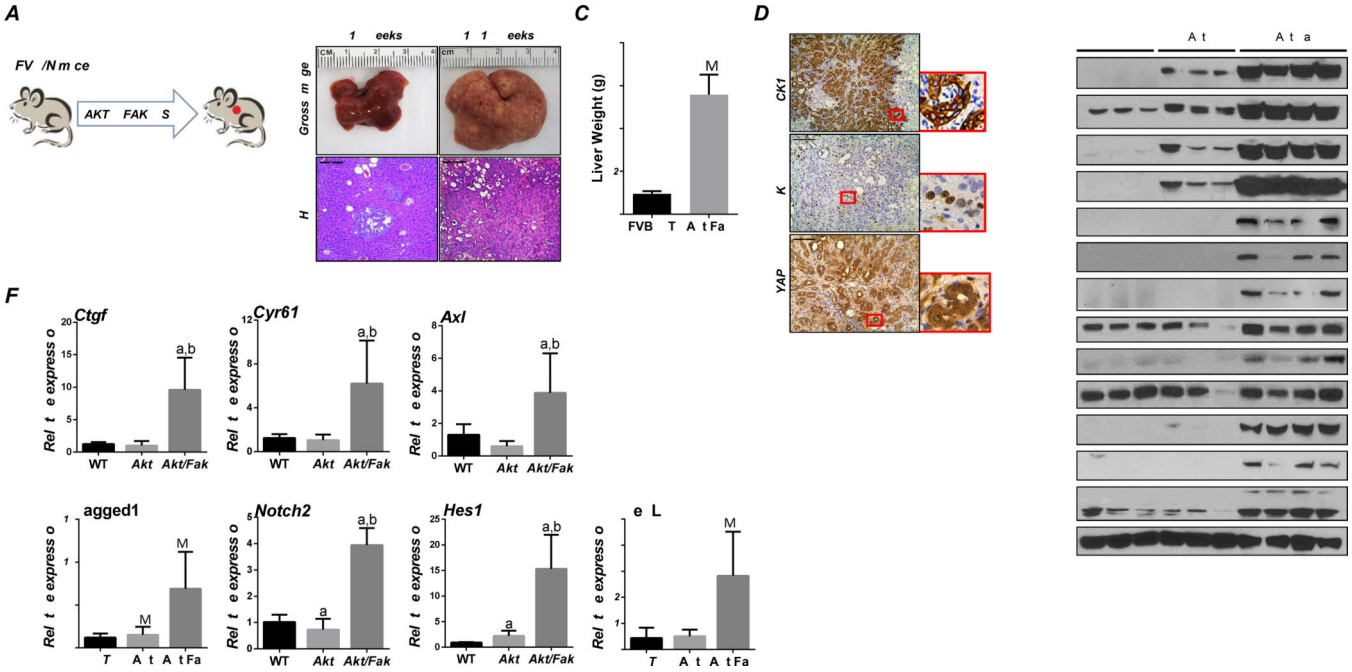

Figure 5. FAK accelerates tumor development in *Akt/Jag 1* mice.

(A) Study design. (B) *Akt/Jag1/pT3* and *Akt/Jag1/Fak* mice's liver weight at ~10 weeks post hydrodynamic injection. (C) Gross image, H&E, CK19, and (D) Ki-67 staining in *Akt/Jag1/PT3* and *Akt/Jag1/Fak* mice. Ki-67 positive cells were quantified using Image J software. (E) Representative Western Blot analysis of relative pathways in *Akt/Jag1/PT3* and *Akt/Jag1/Fak* mice. (F) Immunohistochemistry of YAP in *Akt/Jag1/PT3* and *Akt/Jag1/Fak* mice. (G) YAP and NOTCH signaling activation at the transcriptional level was assessed by qPCR. (H) Study design in $Yap^{f/f}$ mice. (I-J) Liver weight (I) and gross image, H&E, CK19, and Ki-67 staining (J) of *Akt/Jag1/Fak-pCMV* and -*Cre* $Yap^{f/f}$ mice ~9 weeks post-injection. Tukey–Kramer test: at least $P < 0.005$; (G) a, vs WT; b, vs *Akt/Jag1/Fak/pCMV,* (I) a, vs *Akt/Jag1/Fak/pCMV*.

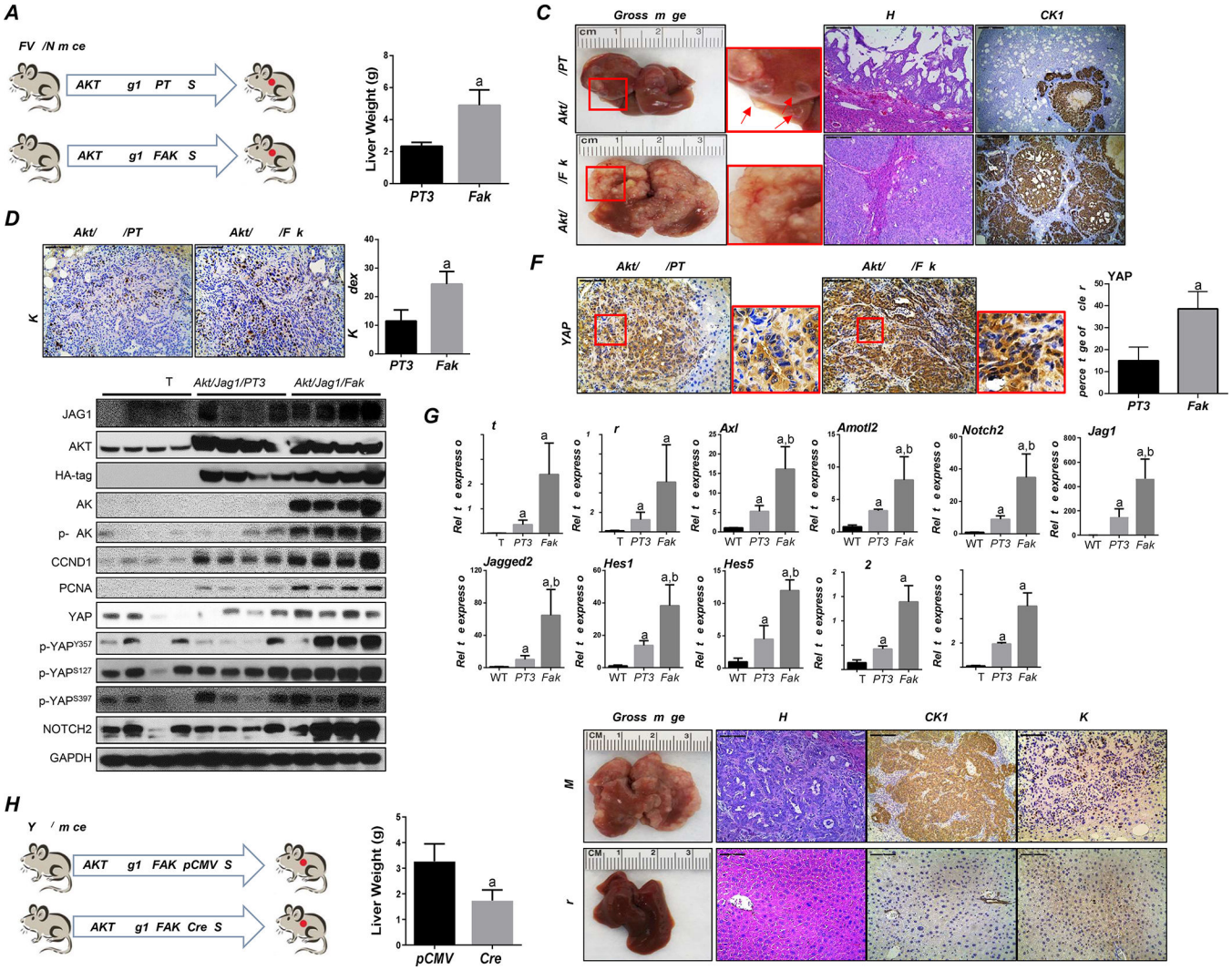

Figure 6. FAK downregulation after tumor formation using the CK19-CreER^{T2} Tamoxifen system inhibits tumor progression.

(A) Study design. (B) Survival analysis of *Fak*$^{f/f}$ mice bearing *Akt/YAP/CreER*^{T2} tumors treated with Tamoxifen or vehicle (Control). (C) Liver weight, (D) Gross image, H&E staining, HNF-4α, and CK19 immunohistochemistry of livers from pretreatment, control, and Tamoxifen groups. Arrows indicate tiny lesions consisting of small cell clusters, which were typically conserved in Tamoxifen-treated mice. (E) FAK Western blot analysis was performed in *Fak*$^{f/f}$ mice bearing *Akt/YAP/CreER*^{T2} tumors sensitized with Tamoxifen (Group2 in C) or not (Group1 in C). (F) Large areas of necrosis (N) in livers from Group2 mice, as shown at two magnifications. Abbreviations: T, tumor; ST, surrounding tissue.

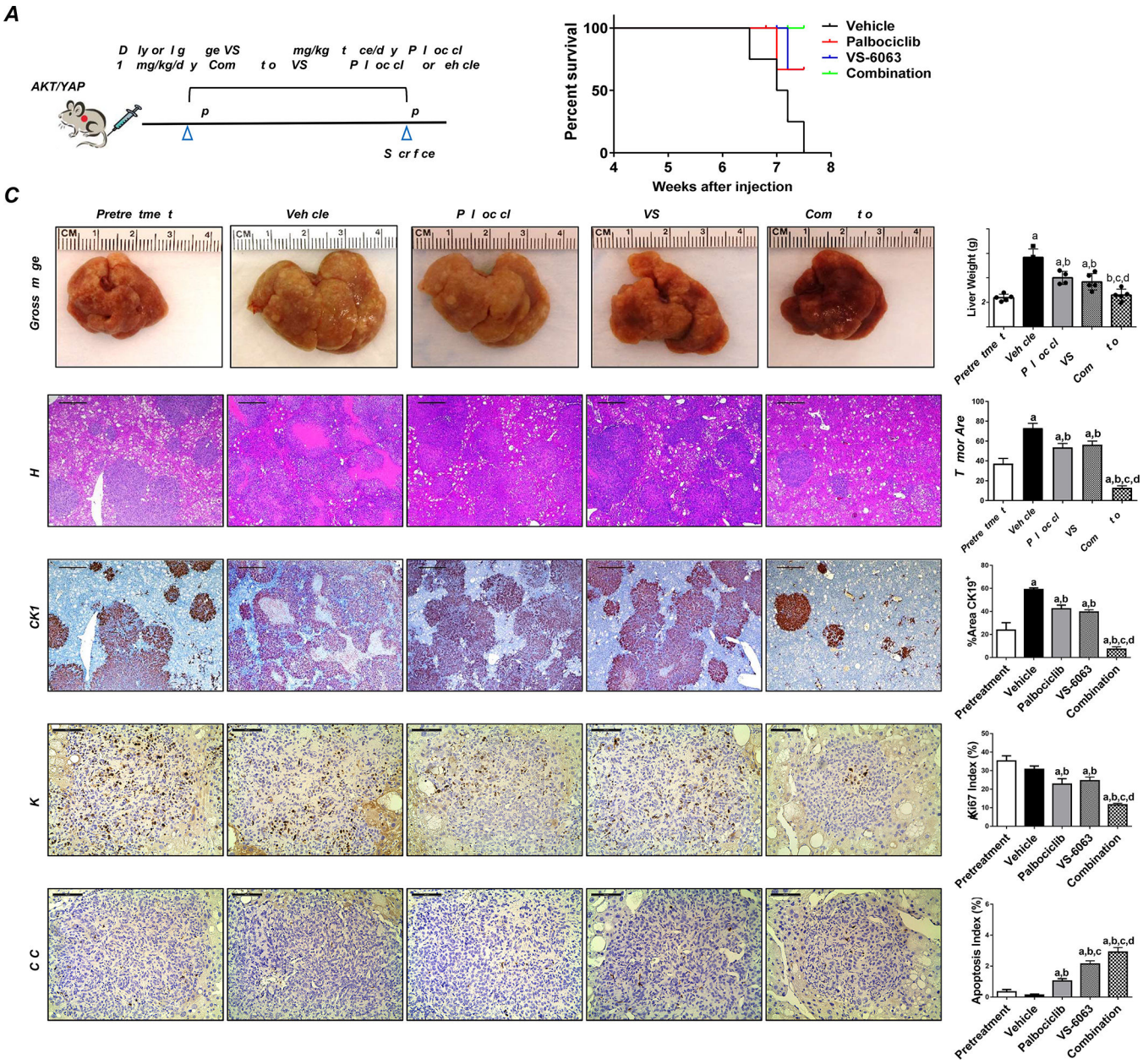

Figure 7. Combining FAK inhibitor VS-6063 and Palbociclib has potent anti-neoplastic activity in iCCA lesions from *Akt/YAP* mice.

(A) Study design. (B) Survival curve, (C) Gross images and H&E, Ki-67, CK19, and C-C-3 staining of livers from pretreatment, vehicle-, VS-6063-, Palbociclib-, and VS-6063/Palbociclib-treated *Akt/YAP* mice. Asterisks indicate necrotic areas. H&E, CK19: Magnification ×40; scale bar =500μm. Ki-67, C-C-3: Magnification ×200; scale bar =100μm. CK19 positive staining, tumor area on H&E-stained slides, Ki-67, and C-C-3–positive cells were counted and quantified by Image J software. Tukey–Kramer test: at least $P < 0.05$. a, vs. Pretreatment; b, vs. Vehicle; c, vs. Palbociclib; d, vs. VS-6063. Abbreviations: C-C-3, cleaved caspase 3.